

Singlet fermionic dark matter

Kang Young Lee

Department of Physics, Korea University, Seoul 136-701, Korea
E-mail: kylee@muon.kaist.ac.kr

Yeong Gyun Kim, Seodong Shin

Department of Physics, KAIST, Daejeon 305-701, Korea
E-mail: ygkim@muon.kaist.ac.kr, sshin@muon.kaist.ac.kr

ABSTRACT: We propose a renormalizable model of a fermionic dark matter by introducing a gauge singlet Dirac fermion and a real singlet scalar. The bridges between the singlet sector and the standard model sector are only the singlet scalar interaction terms with the standard model Higgs field. The singlet fermion couples to the standard model particles through the mixing between the standard model Higgs and singlet scalar and is naturally a weakly interacting massive particle (WIMP). The measured relic abundance can be explained by the singlet fermionic dark matter as the WIMP within this model. Collider implication of the singlet fermionic dark matter is also discussed. Predicted is the elastic scattering cross section of the singlet fermion into target nuclei for a direct detection of the dark matter. Search of the direct detection of the dark matter provides severe constraints on the parameters of our model.

KEYWORDS: cold dark matter, singlet fermion, singlet scalar.

Contents

1. Introduction	1
2. The Model	2
3. Implications in cosmology and collider physics	4
4. Direct detection	8
5. Conclusion	10

1. Introduction

The missing mass of some non-visible form of matter in the galaxy cluster was first investigated by Zwicky in 1933 [1]. Since then, there have been a lot of efforts to probe the dark matter (DM) which provides the unseen mass in the cluster. Evidences have been found including the galactic rotation curve [2] and the observation of the Bullet cluster [3]. The precise measurement of the relic abundance of the cold dark matter (CDM) has been obtained from the Wilkinson microwave anisotropy probe (WMAP) data on the cosmic microwave background radiation as [4]

$$0.085 < \Omega_{CDM}h^2 < 0.119, \quad (2\sigma \text{ level}) \quad (1.1)$$

where Ω is the normalized relic density and the scaled Hubble constant $h \approx 0.7$ in the units of 100 km/sec/Mpc.

Since there is no proper CDM candidate in the standard model (SM) contents, the extended models of the SM are required to provide a candidate of DM. Various candidates of the CDM have been proposed. Weakly interacting massive particles (WIMP) are favored to explain the observed value of the relic abundance in view of new physics beyond the SM. WIMPs include the lightest supersymmetric particle (LSP) in the supersymmetric models with R parity [5, 6], the lightest Kaluza-Klein particle in the extra dimensional models with conserved KK parity [7], and the lightest T-odd particle in the T-parity conserved little Higgs model [8]. Addition of a real singlet scalar field to the SM with Z_2 -parity has been considered as one of the simplest extensions of the SM with the nonbaryonic CDM [9, 10, 11]. Another scalar extension with multiple Higgs doublets is presented in Ref. [12]. General classification of the extra gauge multiplets as a minimal dark matter candidate has been performed in Ref. [13]. On the other hand, incorporating the gauge coupling unification with the dark matter issue, a fermionic DM with the quantum numbers of SUSY higgsinos and a singlet is suggested [14]. A model with a gauge singlet Dirac fermion

is proposed as a minimal model of fermionic dark matter[15]. In this model, the singlet fermion interacts with the SM sector only through nonrenormalizable interactions among which the leading interaction term is given by the dimension five term $(1/\Lambda)H^\dagger H\bar{\psi}\psi$, where H is the SM Higgs doublet and ψ is the dark matter fermion, suppressed by a new physics scale Λ .

We propose a renormalizable extension of the SM with a hidden sector which consists of SM gauge singlets (a singlet scalar and a singlet fermion). The singlet scalar interacts with the SM sector through the triple and quartic scalar interactions. There are no renormalizable interaction terms between the singlet fermion and the SM particles but the singlet fermion interacts with the SM matters only via the singlet scalar. Therefore it is natural that the singlet fermion is a WIMP and a candidate of the CDM. Our model is a minimal model of renormalizable extension of the SM including the fermionic dark matter. The model is described in section 2. We show that the singlet fermion can be a CDM candidate, which explains the measured relic density by the WMAP with the experimental constraint on the Higgs bosons at LEP2 in section 3. The direct detection of the fermionic CDM is investigated in Sec.4. Finally we conclude in Sec.5.

2. The Model

We introduce a hidden sector consisting of a real scalar field S and a Dirac fermion field ψ which are SM gauge singlets. The singlet scalar S couples to the SM particles only through triple and quartic terms with the SM Higgs boson such as $SH^\dagger H$ and $S^2H^\dagger H$. No renormalizable interacting terms between the singlet fermion ψ and the SM particles are allowed. Thus the interaction of ψ with the SM particles just comes via the singlet scalar.

We write the Lagrangian as

$$\mathcal{L} = \mathcal{L}_{SM} + \mathcal{L}_{hid} + \mathcal{L}_{int}, \tag{2.1}$$

where the hidden sector Lagrangian is given by

$$\mathcal{L}_{hid} = \mathcal{L}_S + \mathcal{L}_\psi - g_S\bar{\psi}\psi S, \tag{2.2}$$

with

$$\begin{aligned} \mathcal{L}_S &= \frac{1}{2}(\partial_\mu S)(\partial^\mu S) - \frac{m_0^2}{2}S^2 - \frac{\lambda_3}{3!}S^3 - \frac{\lambda_4}{4!}S^4, \\ \mathcal{L}_\psi &= \bar{\psi}(i\cancel{\partial} - m_{\psi_0})\psi. \end{aligned} \tag{2.3}$$

The interaction Lagrangian between the hidden sector and the SM fields is given by

$$\mathcal{L}_{int} = -\lambda_1 H^\dagger H S - \lambda_2 H^\dagger H S^2. \tag{2.4}$$

The scalar potential given in Eq. (2.3) and (2.4) together with the SM Higgs potential $-\mu^2 H^\dagger H + \bar{\lambda}_0(H^\dagger H)^2$ derives the vacuum expectation values (VEVs)

$$\langle H \rangle = \frac{1}{\sqrt{2}} \begin{pmatrix} 0 \\ v_0 \end{pmatrix} \tag{2.5}$$

for the SM Higgs doublet to give rise to the electroweak symmetry breaking, and $\langle S \rangle = x_0$ for the singlet scalar sector. The extremum conditions $\partial V/\partial H|_{\langle H^0 \rangle = v_0/\sqrt{2}} = 0$ and $\partial V/\partial S|_{\langle S \rangle = x_0} = 0$ lead to the relations [16]

$$\begin{aligned}\mu^2 &= \bar{\lambda}_0 v_0^2 + (\lambda_1 + \lambda_2 x_0)x_0, \\ m_0^2 &= -\frac{\lambda_3}{2}x_0 - \frac{\lambda_4}{6}x_0^2 - \frac{\lambda_1 v_0^2}{2x_0} - \lambda_2 v_0^2.\end{aligned}\quad (2.6)$$

The neutral scalar states h and s defined by $H^0 = (v_0 + h)/\sqrt{2}$ and $S = x_0 + s$ are mixed to yield the mass matrix given by

$$\begin{aligned}\mu_h^2 &\equiv \left. \frac{\partial^2 V}{\partial h^2} \right|_{h=s=0} = 2\bar{\lambda}_0 v_0^2, \\ \mu_s^2 &\equiv \left. \frac{\partial^2 V}{\partial s^2} \right|_{h=s=0} = \frac{\lambda_3}{2}x_0 + \frac{\lambda_4}{3}x_0^2 - \frac{\lambda_1 v_0^2}{2x_0}, \\ \mu_{hs}^2 &\equiv \left. \frac{\partial^2 V}{\partial h \partial s} \right|_{h=s=0} = (\lambda_1 + 2\lambda_2 x_0)v_0.\end{aligned}\quad (2.7)$$

The mass eigenstates h_1 and h_2 are obtained by

$$\begin{aligned}h_1 &= \sin \theta s + \cos \theta h, \\ h_2 &= \cos \theta s - \sin \theta h,\end{aligned}\quad (2.8)$$

where the mixing angle θ is defined by

$$\tan \theta = \frac{y}{1 + \sqrt{1 + y^2}},\quad (2.9)$$

with $y \equiv 2\mu_{hs}^2/(\mu_h^2 - \mu_s^2)$. The Higgs boson masses m_1 and m_2 are given by

$$m_{1,2}^2 = \frac{\mu_h^2 + \mu_s^2}{2} \pm \frac{\mu_h^2 - \mu_s^2}{2} \sqrt{1 + y^2},\quad (2.10)$$

where the upper (lower) sign corresponds to m_1 (m_2). According to the definition of $\tan \theta$, we get $|\cos \theta| > \frac{1}{\sqrt{2}}$ implying that h_1 is SM Higgs-like while h_2 is the singlet-like scalars. As a result, there exist two neutral Higgs bosons in our model and the collider phenomenology of the Higgs sector might be affected. We will discuss it in later section.

The singlet fermion ψ has the mass $m_\psi = m_{\psi_0} + g_S x_0$ as an independent parameter of the model since m_{ψ_0} is just a free parameter. The Yukawa coupling g_S measures the interaction of ψ with other particles. Generically the interactions between ψ and the SM particles are suppressed by the mass of singlet scalar and/or the Higgs mixing. Therefore ψ is naturally weakly interacting and can play the role of a cold dark matter as a WIMP. If we fix masses of two Higgs bosons, the singlet fermion annihilation processes into the SM particles depend upon the fermion mass m_ψ , Yukawa coupling g_S , and the Higgs mixing angle θ . If the final state includes Higgs bosons, h_1 or h_2 , several Higgs self-couplings are involved depending on various couplings in the scalar potential.

3. Implications in cosmology and collider physics

In the early universe, the dark matter is assumed to be in thermal equilibrium by the active annihilation and production process with the SM sector. When the universe cools down and the temperature T drops below the DM mass, the DM number density is suppressed exponentially so that the annihilation rate of the dark matter becomes smaller than even the Hubble parameter. Then the interactions of the DM freeze out to make the DM particles fall out of equilibrium and the DM number density in a comoving volume remains constant. Therefore the current relic abundance of the CDM depends on the annihilation cross section of ψ into the SM particles or the additional Higgs bosons in our model. The pair annihilation process of ψ consists of the annihilation into SM particles via Higgs-mediated s -channel processes and into Higgs bosons via s , t , and u -channels. The dominant final states of the SM particles are $b\bar{b}$, $t\bar{t}$, W^+W^- , and ZZ . The total cross section of the annihilation process is given by

$$\sigma_{v_{rel}} = \frac{(g_S \sin \theta \cos \theta)^2}{16\pi} \left(1 - \frac{4m_\psi^2}{\mathfrak{s}} \right) \quad (3.1)$$

$$\times \left(\frac{1}{(\mathfrak{s} - m_{h_1}^2)^2 + m_{h_1}^2 \Gamma_{h_1}^2} + \frac{1}{(\mathfrak{s} - m_{h_2}^2)^2 + m_{h_2}^2 \Gamma_{h_2}^2} \right) \quad (3.2)$$

$$- \frac{2(\mathfrak{s} - m_{h_1}^2)(\mathfrak{s} - m_{h_2}^2) + 2m_{h_1}m_{h_2}\Gamma_{h_1}\Gamma_{h_2}}{((\mathfrak{s} - m_{h_1}^2)^2 + m_{h_1}^2 \Gamma_{h_1}^2)((\mathfrak{s} - m_{h_2}^2)^2 + m_{h_2}^2 \Gamma_{h_2}^2)} \quad (3.3)$$

$$\times \left[\left(\frac{m_b}{v_0} \right)^2 \cdot 2\mathfrak{s} \left(1 - \frac{4m_b^2}{\mathfrak{s}} \right)^{3/2} \cdot 3 + \left(\frac{m_t}{v_0} \right)^2 \cdot 2\mathfrak{s} \left(1 - \frac{4m_t^2}{\mathfrak{s}} \right)^{3/2} \cdot 3 \right] \quad (3.4)$$

$$+ \left(2 \frac{m_W^2}{v_0} \right)^2 \left(2 + \frac{(\mathfrak{s} - 2m_W^2)^2}{4m_W^4} \right) \cdot \sqrt{1 - \frac{4m_W^2}{\mathfrak{s}}} \quad (3.5)$$

$$+ \left(2 \frac{m_Z^2}{v_0} \right)^2 \left(2 + \frac{(\mathfrak{s} - 2m_Z^2)^2}{4m_Z^4} \right) \cdot \sqrt{1 - \frac{4m_Z^2}{\mathfrak{s}}} \cdot \frac{1}{2} \quad (3.6)$$

$$+ \sum_{i,j=1,2} \sigma_{h_i h_j} + \sum_{i,j,k=1,2} \sigma_{h_i h_j h_k}, \quad (3.7)$$

where Γ_{h_i} is the decay width of h_i for $i = 1, 2$, and $\sigma_{h_i h_j}$, $\sigma_{h_i h_j h_k}$ are the annihilation cross sections of $\bar{\psi}\psi$ into $h_i h_j$ or $h_i h_j h_k$ with $i, j, k = 1, 2$. Here, $\sqrt{\mathfrak{s}}$ denotes the center of mass energy. The thermal average of the cross section over \mathfrak{s} is given by

$$\langle \sigma_{ann.v_{rel}} \rangle = \frac{1}{8m_\psi^4 T K_2^2(m_\psi/T)} \int_{4m_\psi^2}^{\infty} d\mathfrak{s} \sigma_{ann.}(\mathfrak{s}) (\mathfrak{s} - 4m_\psi^2) \sqrt{\mathfrak{s}} K_1 \left(\frac{\sqrt{\mathfrak{s}}}{T} \right), \quad (3.8)$$

where $K_{1,2}$ are the modified Bessel functions. The evolution of the number density of the singlet fermion is described by the Boltzmann equation in terms of $\langle \sigma_{ann.v_{rel}} \rangle$ and the equilibrium number density of ψ

$$\frac{dn_\psi}{dt} + 3Hn_\psi = -\langle \sigma_{ann.v_{rel}} \rangle \left[n_\psi^2 - \left(n_\psi^{EQ} \right)^2 \right], \quad (3.9)$$

where H is the Hubble parameter and n_ψ^{EQ} is the equilibrium number density of ψ . After the freeze out of the annihilation processes, the actual number of ψ per comoving volume becomes constant and the present relic density $\rho_\psi = m_\psi n_\psi$ is determined. The freeze-out condition gives the thermal relic density in terms of the thermal average of the annihilation cross section.

$$\Omega_\psi h^2 \approx \frac{(1.07 \times 10^9)x_F}{\sqrt{g_*} M_{pl}(GeV) \langle \sigma_{ann} v_{rel} \rangle}, \tag{3.10}$$

where g_* counts the effective degrees of freedom of the relativistic quantities in equilibrium. The inverse freeze-out temperature $x_F = m_\psi/T_F$ is determined by the iterative equation

$$x_F = \log \left(\frac{m_\psi}{2\pi^3} \sqrt{\frac{45 M_{pl}^2}{2g_* x_F} \langle \sigma_{ann} v_{rel} \rangle} \right). \tag{3.11}$$

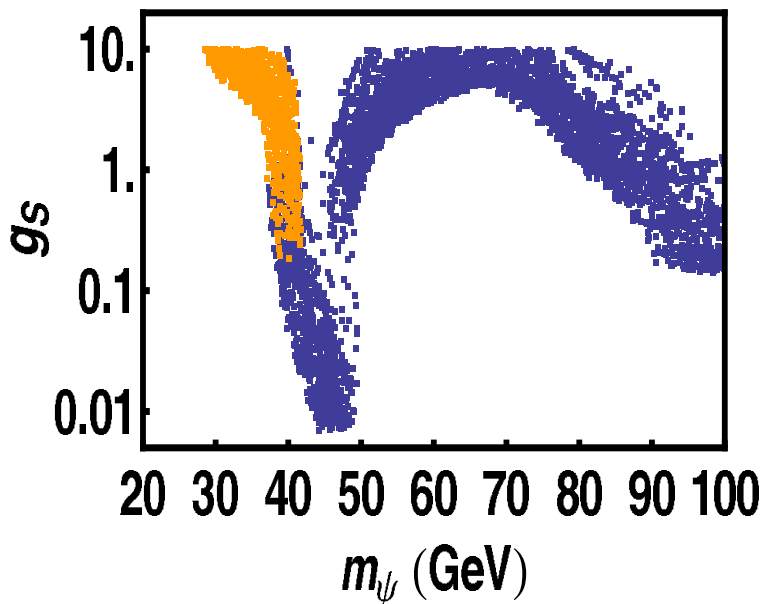


Figure 1: Allowed parameter set of (m_ψ, g_S) with $m_{h_1} = 90$ GeV ($\pm 1\%$) and $m_{h_2} = 500$ GeV ($\pm 12\%$). The allowed region by LEP2 data is denoted as orange region.

We investigate the allowed model parameter space, which provide thermal relic density consistent with the WMAP observation. In addition to m_ψ and g_S , we have six more undetermined parameters in the scalar potential: $\bar{\lambda}_0, \lambda_1, \lambda_2, \lambda_3, \lambda_4, x_0$, which determine the Higgs boson masses (m_{h_1}, m_{h_2}), mixing angle (θ), and triple and quartic self couplings of Higgs bosons. Here we have to study a large volume of the multidimensional parameter space. For clarity of the presentation of our result, we fix the Higgs masses, m_{h_1} and m_{h_2} within some ranges, while allowing the other parameters such as Higgs mixing angle and self couplings vary freely. Our parameter sets should satisfy several physical conditions. We demand that *i*) the potential is bounded from below, *ii*) the electroweak symmetry breaking is viable, and *iii*) all couplings keep the perturbativity.

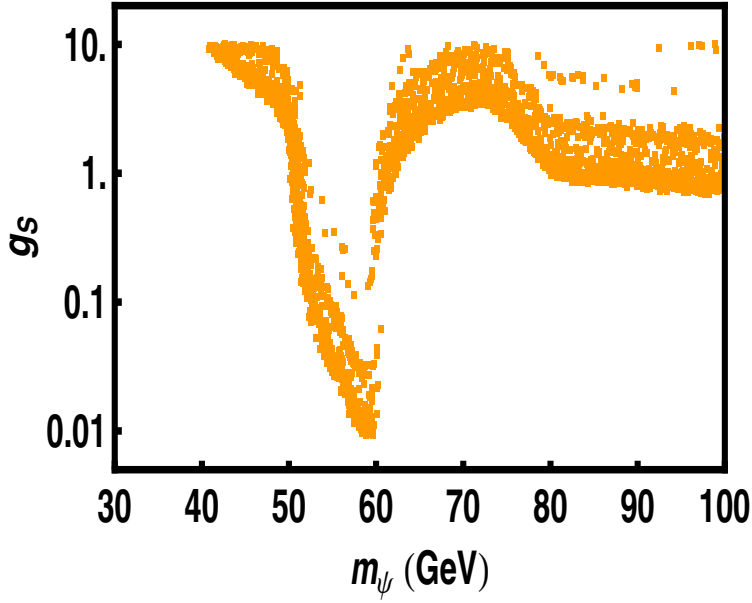


Figure 2: Allowed parameter set of (m_ψ, g_S) with $m_{h_1} = 120 \text{ GeV}$ ($\pm 1\%$) and $m_{h_2} = 500 \text{ GeV}$ ($\pm 12\%$). The allowed region by LEP2 data is denoted as orange region.

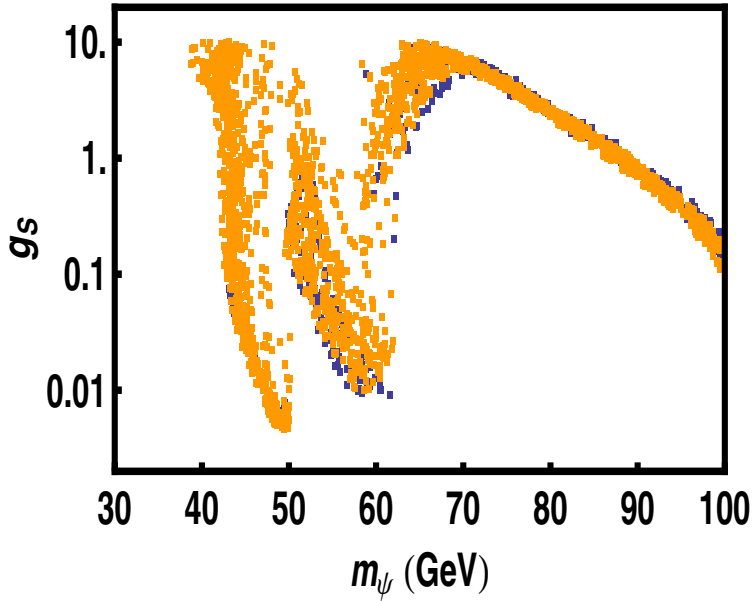


Figure 3: Allowed parameter set of (m_ψ, g_S) with $m_{h_1} = 120 \text{ GeV}$ ($\pm 4\%$) and $m_{h_2} = 100 \text{ GeV}$ ($\pm 1\%$). The allowed region by LEP2 data is denoted as orange region.

Fig.1 shows the allowed parameter set by the measured relic abundance with $m_{h_1} = 90 \text{ GeV}$ ($\pm 1\%$) and $m_{h_2} = 500 \text{ GeV}$ ($\pm 12\%$). The valley in Fig.1 implies the resonant region of h_1 exchange for DM pair annihilation, where $2m_\psi \simeq m_{h_1}$. The coupling constant g_S should be small in that region in order to compensate the enhancement of the cross section due to the Higgs resonance effect. A step appears when $m_\psi \sim 80 \text{ GeV}$, which denotes that

the annihilation channel $\bar{\psi}\psi \rightarrow W^-W^+/ZZ$ opens as m_ψ exceeds the W and Z boson masses.

The current experimental bound on Higgs mass can have a significant impact on the allowed parameter space. Note that the LEP2 bound of the SM Higgs boson mass gets weaker in our model since the SM-like Higgs couplings are modified, and therefore $m_{h_1} = 90$ GeV might be allowed depending on the parameter set. The promising channel to produce a neutral Higgs boson at LEP is the Higgs-strahlung process, $e^-e^+ \rightarrow Zh$. A lower bound on the mass of the SM Higgs boson has been established to be 114.4 GeV at 95 % confidence level [17]. In our model, the Higgs mixing alters the h_iZZ couplings and therefore the cross sections of the Higgs-strahlung processes. Furthermore, Higgses can invisibly decay to a pair of singlet fermions. Thus the SM bound should be modified accordingly. We consider the parameters defined by

$$\xi_i^2 = \left(\frac{g_{h_iZZ}}{g_{HZZ}^{SM}} \right)^2 \frac{\Gamma_{h_i}^{SM}}{\Gamma_{h_i}^{SM} + \Gamma(h_i \rightarrow \bar{\psi}\psi)}, \quad (3.12)$$

where $\Gamma_{h_i}^{SM}$ are the widths of h_i decays into the SM particles. Assuming the non-standard models, the lower bound on the Higgs mass is represented by the upper bound of ξ_i^2 , which is shown in Ref. [17]. In our analysis, we impose $\xi^2 < 0.1$ as a conservative bound for $m_{h_i} = 90$ GeV (and $\xi^2 < 0.3$ for $m_{h_i} = 100$ GeV for later use). Since a new fermion exists in our model, the definition of ξ^2 includes the decay width for invisible decay channel, $h_i \rightarrow \bar{\psi}\psi$. On the figure, the orange points denote the region which satisfy the Higgs mass bound. The allowed region appears when $m_\psi \lesssim m_{h_1}/2$, due to large contribution from the invisible Higgs decay. If $m_\psi > m_{h_1}/2$, the decay channel $h_1 \rightarrow \bar{\psi}\psi$ is closed and $\xi_1^2 = (\cos\theta)^2$ is always larger than 0.1 so that the corresponding region is excluded by the experimental results of LEP2.

Allowed parameter set with $m_{h_1} = 120$ GeV and $m_{h_2} = 500$ GeV are shown in Fig.2. This parameter set always satisfy the LEP2 constraints on the Higgs boson mass, because the Higgs masses are larger than the current experimental bound.

Fig.3 shows the allowed parameter set for $m_{h_1} = 120$ GeV and $m_{h_2} = 100$ GeV. Here m_{h_1} and m_{h_2} are comparable and there are two resonant regions corresponding to h_1 and h_2 resonances. One can notice that the most of parameter points also satisfy the Higgs mass bound.

We now briefly comment on possible LHC phenomenology of our model. One obvious difference of the model from SM is that we have two neutral Higgs bosons which have smaller couplings to SM particles, compared to SM Higgs case. Other characteristic of the model is that the Higgs bosons can decay invisibly to a pair of singlet fermions, if kinematically allowed. Fig. 4 shows the ratio of $\Gamma_{h_1}^{SM}$ to the total decay width of h_1 , for $m_{h_1} = 120$ GeV and $m_{h_2} = 500$ GeV. We have very large invisible branching ratios when the mass of singlet fermion is less than half of m_{h_1} . Such a large invisible Higgs decay may be observed at the CERN LHC [18, 19].

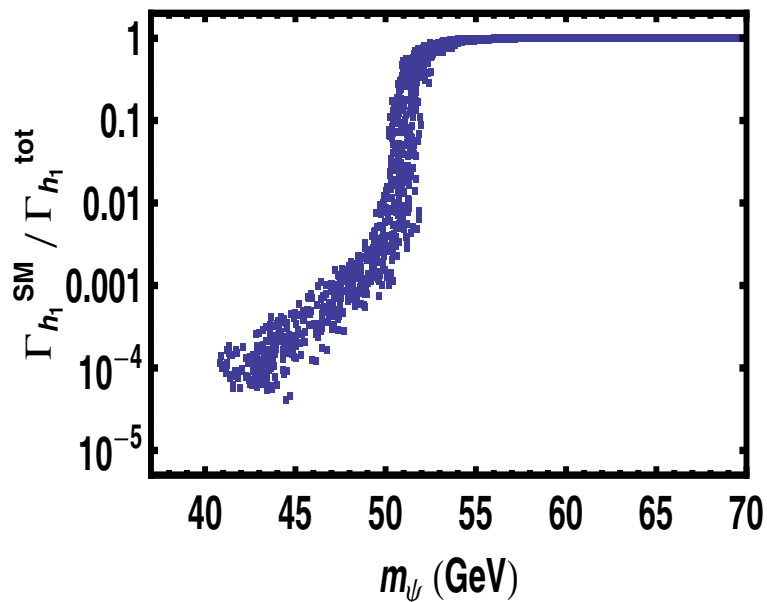


Figure 4: The ratio of $\Gamma_{h_1}^{SM}$ to the total decay width of h_1 with $m_{h_1} = 120$ GeV ($\pm 1\%$) and $m_{h_2} = 500$ GeV ($\pm 12\%$).

4. Direct detection

There are several experiments to detect the WIMP directly through the elastic scattering of the WIMP on the target nuclei [20, 21]. The effective Lagrangian describing the elastic scattering of the WIMP and a nucleon is given by

$$\mathcal{L}_{eff} = f_p(\bar{\psi}\psi)(p\bar{p}) + f_n(\bar{\psi}\psi)(n\bar{n}), \quad (4.1)$$

where the coupling constant f_p is given by [22, 23]

$$\frac{f_{p,n}}{m_{p,n}} = \sum_{q=u,d,s} f_{Tq}^{(p,n)} \frac{\alpha_q}{m_q} + \frac{2}{27} f_{Tg}^{(p,n)} \sum_{q=c,b,t} \frac{\alpha_q}{m_q}, \quad (4.2)$$

with the matrix elements $m_{(p,n)} f_{Tq}^{(p,n)} \equiv \langle p, n | m_q \bar{q}q | p, n \rangle$ for $q = u, d, s$ and $f_{Tg}^{(p,n)} = 1 - \sum_{q=u,d,s} f_{Tq}^{(p,n)}$. The numerical values of the hadronic matrix elements $f_{Tq}^{(p,n)}$ are determined in Ref. [23]

$$f_{Tu}^{(p)} = 0.020 \pm 0.004, \quad f_{Td}^{(p)} = 0.026 \pm 0.005, \quad f_{Ts}^{(p)} = 0.118 \pm 0.062, \quad (4.3)$$

and

$$f_{Tu}^{(n)} = 0.014 \pm 0.003, \quad f_{Td}^{(n)} = 0.036 \pm 0.008, \quad f_{Ts}^{(n)} = 0.118 \pm 0.062. \quad (4.4)$$

Since $f_{Ts}^{(p,n)}$ dominantly contributes to $f_{(p,n)}$, we let $f_p \approx f_n$. The effective coupling constant α_q is defined by the spin-independent four fermion interaction of the quarks and

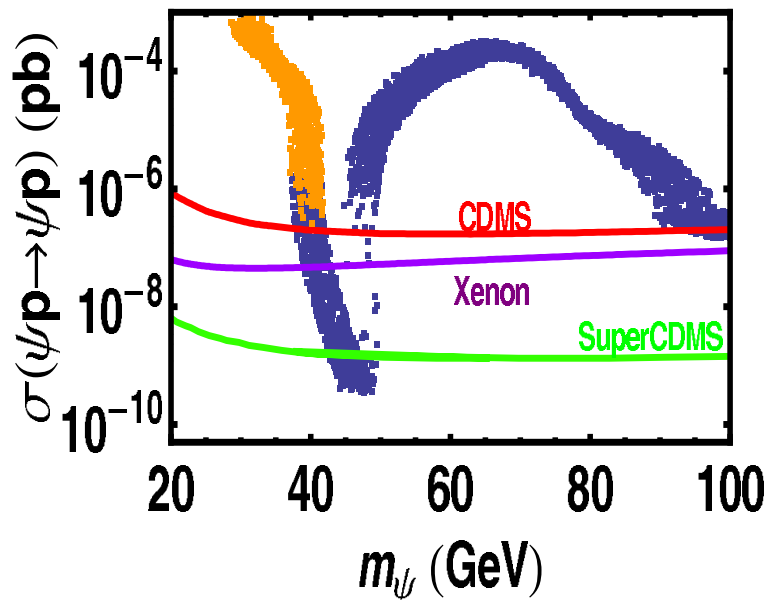


Figure 5: Predictions of the elastic scattering cross section $\sigma(\psi p \rightarrow \psi p)$ with respect to m_ψ with $m_{h_1} = 90$ GeV ($\pm 1\%$) and $m_{h_2} = 500$ GeV ($\pm 12\%$). The red line indicates the CDMS bound, the purple line the Xenon bound, and the green line the up-coming super CDMS bound. The allowed region by LEP2 data is denoted as orange region.

the dark matter fermion in this model. The effective Lagrangian is given by

$$\mathcal{L}_{int} = \sum_q \alpha_q (\bar{\psi}\psi)(\bar{q}q), \quad (4.5)$$

where α_q is derived by the Higgs exchange t -channel diagram to be determined by

$$\alpha_q = \frac{g_S \sin \theta \cos \theta m_q}{v_0} \left(\frac{1}{m_{h_1}^2} - \frac{1}{m_{h_2}^2} \right). \quad (4.6)$$

The elastic scattering cross section is obtained from the effective Lagrangian (4.1)

$$\sigma = \frac{4M_r^2}{\pi} [Z f_p + (A - Z) f_n]^2 \approx \frac{4M_r^2 A^2}{\pi} f_p^2, \quad (4.7)$$

where M_r is the reduced mass defined by $1/M_r = 1/m_\psi + 1/m_{nuclei}$. For the convenience of being compared with the experiments, we obtain the cross section with the single nucleon given by

$$\sigma(\psi p \rightarrow \psi p) \approx \frac{4m_r^2}{\pi} f_p^2, \quad (4.8)$$

where m_r is the reduced mass given by $1/m_r = 1/m_\psi + 1/m_p$.

The prediction of the elastic scattering cross sections with the allowed parameter set as in Fig.1 is depicted in Fig.5. Allowed parameter sets by the LEP2 data are again denoted by orange points on the figure. The allowed region is entirely excluded by the current experiments including CDMS [24] and Xenon[25].

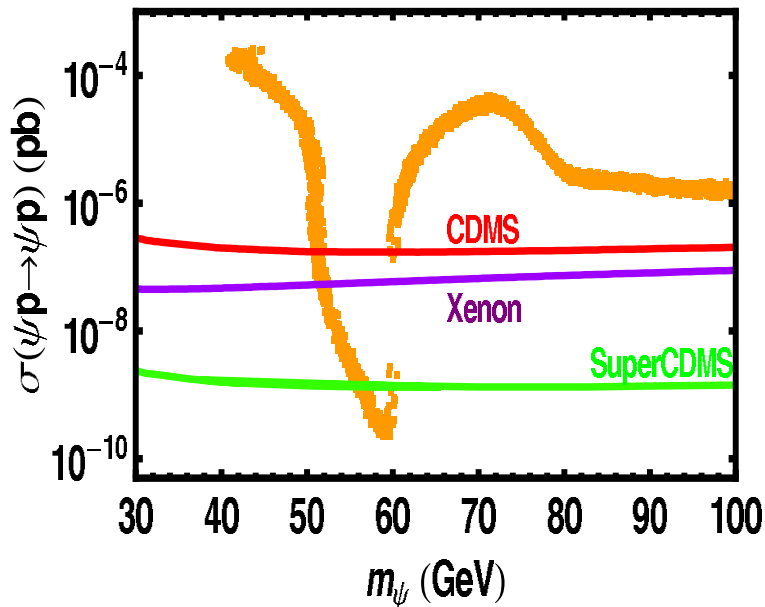


Figure 6: Predictions of the elastic scattering cross section $\sigma(\psi p \rightarrow \psi p)$ with respect to m_ψ with $m_{h_1} = 120$ GeV ($\pm 1\%$) and $m_{h_2} = 500$ GeV ($\pm 12\%$). The red line indicates the CDMS bound, the purple line the Xenon bound, and the green line the up-coming super CDMS bound. The allowed region by LEP2 data is denoted as orange region.

The cross sections with the allowed parameter set of Fig.2 and Fig.3 are also depicted in Fig.6 and Fig.7, respectively. The resonance region represented by a valley is not excluded by the experiments up to date. The large m_ψ region in Fig.7 is also still allowed. We expect that the super CDMS experiment in the future will probe the most region of the parameter set for the singlet fermionic dark matter.

5. Conclusion

We propose a renormalizable model with a fermionic cold dark matter. A minimal hidden sector consisting of a SM gauge singlet Dirac fermion and a real singlet scalar is introduced. We show that the singlet fermion can be a candidate of the cold dark matter which explain the relic abundance measured by WMAP. The constraints on the masses and couplings at LEP2 are included and the elastic scattering cross sections for the direct detection are predicted. We find that most region of the parameter set will be probed by the direct detection through elastic scatterings of the DM with nuclei in the near future.

Acknowledgments

This work was supported by the KRF Grant funded by the Korean Government (KRF-2005-C00006), the KOSEF Grant (KOSEF R01-2005-000-10404-0), and the Center for High Energy Physics of Kyungpook National University, the BK21 program of Ministry of Education (Y.G.K., S.S.), and the Korea Research Foundation Grant funded by the

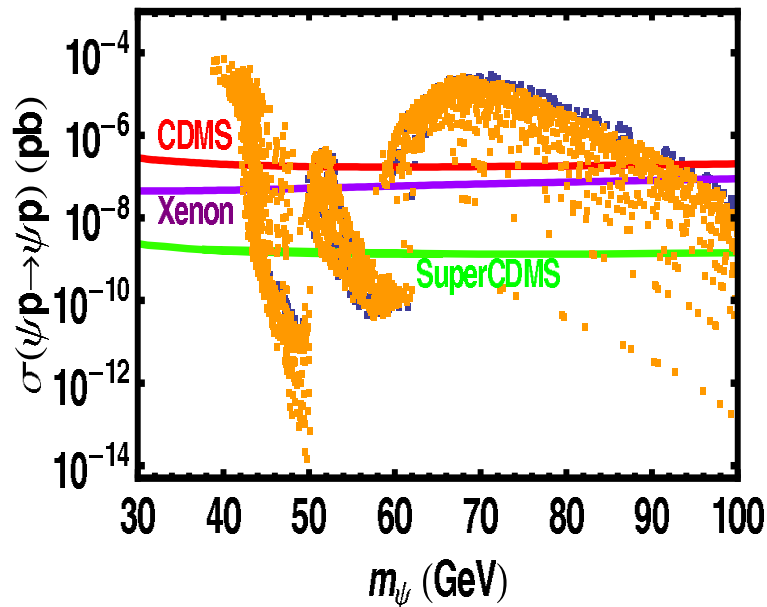


Figure 7: Predictions of the elastic scattering cross section $\sigma(\psi p \rightarrow \psi p)$ with respect to m_ψ with $m_{h_1} = 120$ GeV ($\pm 4\%$) and $m_{h_2} = 100$ GeV ($\pm 1\%$). The red line indicates the CDMS bound, the purple line the Xenon bound, and the green line the up-coming super CDMS bound. The allowed region by LEP2 data is denoted as orange region.

Korean Government (MOEHRD, Basic Research Promotion Fund KRF-2007-C00145) and the BK21 program of Ministry of Education (K.Y.L.). S.S. also thanks to Dr. Junghee Kim for useful discussions on the numerical work.

References

- [1] F. Zwicky, *Helvetica Physica Acta* **6**, 110 (1933); F. Zwicky, *Astrophys. J.* **86**, 217 (1937).
- [2] Y. Sofue and V. Rubin, *Ann. Rev. Astron. Astrophys.* **39**, 137 (2001).
- [3] D. Clowe, M. Bradac, A.H. Gonzalez, M. Markevitch, S.W. Randall, C. Jones and D. Zaritsky, *astro-ph/0608407*.
- [4] C.L. Bennett *et al.*, *Astrophys. J. Suppl. Ser.* **148**, 1 (2003).
- [5] G. Jungman, M. Kamionkowski and K. Griest, *Phys. Rep.* **267**, 195 (1996); G. Bertone, D. Hooper and J. Silk, *Phys. Rep.* **405**, 279 (2005).
- [6] H. Goldberg, *Phys. Rev. Lett.* **50**, 1419 (1983); J. Ellis, J.S. Hagelin, D.V. Nanopoulos, K.A. Olive and M. Srednicki, *Nucl. Phys.* **B238**, 453 (1984); K. Choi, K.Y. Lee, Y. Shimizu, Y.G. Kim and K.-i. Okumura, *JCAP* **0612**, 017 (2006); H. Baer, E.-K. Park, X. Tata and T.T. Wang, *JHEP* **0608**, 041 (2006); T. Moroi, L. Randall, *Nucl. Phys.* **B570**, 455 (2000).
- [7] H.-C. Cheng, J.L. Feng and K.T. Matchev, *Phys. Rev. Lett.* **89**, 211301 (2002); G. Servant and T. Tait, *Nucl. Phys.* **B650**, 391 (2003).
- [8] H.-C. Cheng and I. Low, *JHEP* **0309**, 051 (2003); *JHEP* **0408**, 061 (2004).
- [9] V. Silveira and A. Zee, *Phys. Lett. B* **161**, 136 (1985).

- [10] C.P. Burgess, M. Pospelov and T.ter Veldhuis, Nucl. Phys. **B619**, 709 (2001).
- [11] H. Davoudiasl, R. Kitano, T. Li and H. Murayama, Phys. Lett. B **609**, 117 (2005).
- [12] M. Lisanti and J.G. Wacker, arXiv:0704.2816.
- [13] M. Cirelli, N. Fornengo and A. Strumia, Nucl. Phys. **B753**, 178 (2006).
- [14] R. Mahbubani and L. Senatore, Phys. Rev. D **73**, 043510 (2006).
- [15] Y.G. Kim and K.Y. Lee, Phys. Rev. D **75**, 115012 (2007).
- [16] S. Profumo, M. J. Ramsey-Musolf and G. Shaughnessy, JHEP **0708**, 010 (2007).
- [17] ALEPH collaboration, DELPHI collaboration, L3 Collaboration, OPAL collaboration, The LEP working group for Higgs boson searches, Phys. Lett. B **565**, 61 (2003).
- [18] J. F. Gunion, Phys. Rev. Lett. **72**, 199 (1994).
- [19] O. J. Eboli and D. Zeppenfeld, Phys. Lett. B **495**, 147 (2000).
- [20] M. W. Goodman and E. Witten, Phys. Rev. D **31**, 3059 (1985).
- [21] S. Khali and C. Munoz, Contemporary Physics **43** (2002) 51; C. Munoz, Int. J. Mod. Phys. A **19**, 3093 (2004).
- [22] T. Nihei and M. Sasagawa, Phys. Rev. D **70**, 055011 (2004).
- [23] J. Ellis, A. Ferstl and K.A. Olive, Phys. Lett. B **481**, 304 (2000).
- [24] D. S. Akerib *et al.*, CDMS collaboration, Phys. Rev. Lett. **96**, 011302 (2006).
- [25] J. Angle *et al.*, Xenon collaboration, arXiv:0706.0039